PANIS

ALGORITHM THEORETICAL BASIS DOCUMENT

	Name	Organisation	Date	Visa
Written by:	Alexandre Boughanemi, Julia Pfeffer	Magellium	08/12/2025	
Checked by:	Alejandro Blazquez Hugo Lecomte	CNES LEGOS	15/12/25	
Approved by:	Julia Pfeffer Alejandro Blazquez	Magellium CNES		

Document reference:	SAGSA-DT-003-MAG_ATBD
Edition.Revision:	V1.0
Date Issued:	08/12/2025
Customer:	CNES
Ref. Market, consultation:	MARCHÉ N° 241698/00

Distribution List

	Name	Organisation	No. copies
Sent to :	Alejandro Blazquez & Claude Boniface	CNES	1
Internal copy :	Michaël Ablain	Magellium	1

Document evolution sheet

Ed.	Rev.	Date	Purpose evolution	Comments
V1.0	0	08/12/2025	Submission of the document	First version to be revised by the CNES

Dissemination level

PU	Public	x
PP	Restricted to other programme participants	
RE	Restricted to a group specified by the consortium	
CO	Confidential, only for members of the consortium	

Contents

List of Tables

List of Figures

1. Introduction

1.1. Executive summary

The GRACE (Gravity Recovery And Climate Experiment; (Tapley et al., 2004)) and GRACE-FO (Follow On; (Landerer et al., 2020)) satellite missions provide continuous measurements of Earth's time-variable gravity field, with spatial resolutions on the order of a few hundred kilometers and monthly temporal sampling since April 2002. This long-term record of mass redistribution within the Earth system has transformed our ability to monitor and understand the global water and energy cycles in a changing climate (Chen et al., 2022; Tapley et al., 2019). Deriving quantitative estimates of water-mass variability across the ocean, hydrosphere, and cryosphere, however, requires multiple post-processing corrections informed by diverse geophysical models, analysis centers, and auxiliary datasets. The PANIS software implements an ensemble-based framework that generates surface water-mass anomalies following the historical approach of (Blazquez et al., 2018), enabling the systematic estimation of uncertainties associated with processing and post-processing choices applied to GRACE/GRACE-FO data. Unlike the COST-G framework (Jäggi et al., 2020), which provides uncertainty estimates for Level-2 geopotential products, PANIS focuses on uncertainties in Level-3 surface water-mass anomalies, offering complementary insight for downstream geophysical and climate applications.

1.2. Scope and objectives

The PANIS ATBD (Algorithm Theoretical Basis Document) describes the algorithms used to generate the Level-3 SAGSA ensemble supported by the CNES. The calculation of the ensemble of surface water mass anomaly grids is summarized in Figure 1.

The SAGSA ensemble is based on the Earth's gravitational potential estimated by several production centers, expressed in Stokes coefficients (i.e. in the spherical harmonic basis) up to degree 96, including the JPL (GRACE-FO, 2024), CSR (NASA/JPL, 2023), GFZ (Dahle et al., 2018), ITSG (Kvas et al., 2019), and CNES (J.-M. Lemoine & Bourgogne, 2020). However, such coefficients are affected by several sources of errors and limitations that need to be corrected in several post-processing steps.

- The GRACE and GRACE-FO satellites orbit around the center of mass, therefore are not sensitive to the geocenter motion, and cannot be used to evaluate the Stokes coefficients of degree 1. Three different models are used here to evaluate the geocenter motion (i.e. monthly values of the degree 1 coefficients by (Sun et al., 2016) from three different processing centers).
- The GRACE and GRACE-FO measurements are poorly sensitive to low degrees of the gravity field, in particular the C20 and C30 coefficients. Here, the C20 (full time series) and C30 (after May 2016 only) coefficients estimated by the five processing centers are replaced by more robust SLR measurements from three different data centers (Cheng et al., 2013; J. Lemoine & Reinquin, 2017; Loomis et al., 2019).
- To extract mass variations due to water redistribution with the hydrosphere, ocean and cryosphere, GRACE and GRACE-FO data must be corrected for the ongoing deformations of the visco-elastic Earth due to the previous deglaciation. Two different GIA models are used here (Caron et al., 2018; Peltier et al., 2018). No little ice age (LIA) correction is performed.
- Stokes coefficients are affected by systematic correlated errors, easily identified in the spatial domain as characteristic stripes in the North-South direction. In order to reduce the anisotropic noise, decorrelation filters, called DDK filters (Kusche et al., 2009), are applied to GRACE solutions, using two different orders (DDK3 and DDK6) corresponding to two different levels of filtering.

The combination of five different processing centers, three geocenter models, three oblateness values (C20, C30), two GIA models and two levels of filtering leads to an ensemble of 180 solutions. Additional corrections are applied to all ensemble members in an identical way.

- An earthquake correction is applied to remove the co-seismic deformation of major earthquakes.
- A leakage correction is applied on filtered residuals near the coast, displacing mass anomalies from the ocean to the near land. The leakage correction is based on the modeling of near-coast ocean as “region-wise” constant value for each time (Lecomte et al., 2025)
- Ocean dealiasing models are restored using the GAB model from AOD1B RL06 (Dobslaw et al., 2017). Details about special cases (i.e. the CNES during the GRACE period) are given in section 4.8.3. . The gravitational potentials are corrected to compensate for the total amount of water vapor in the atmosphere expressed in C0 GAA, in order to ensure the conservation of mass at global scale (Chen et al., 2019).

This approach yields an ensemble of 180 solutions, consisting of monthly gridded surface mass anomalies, expressed as equivalent water heights over regular 1°x1° global grids.

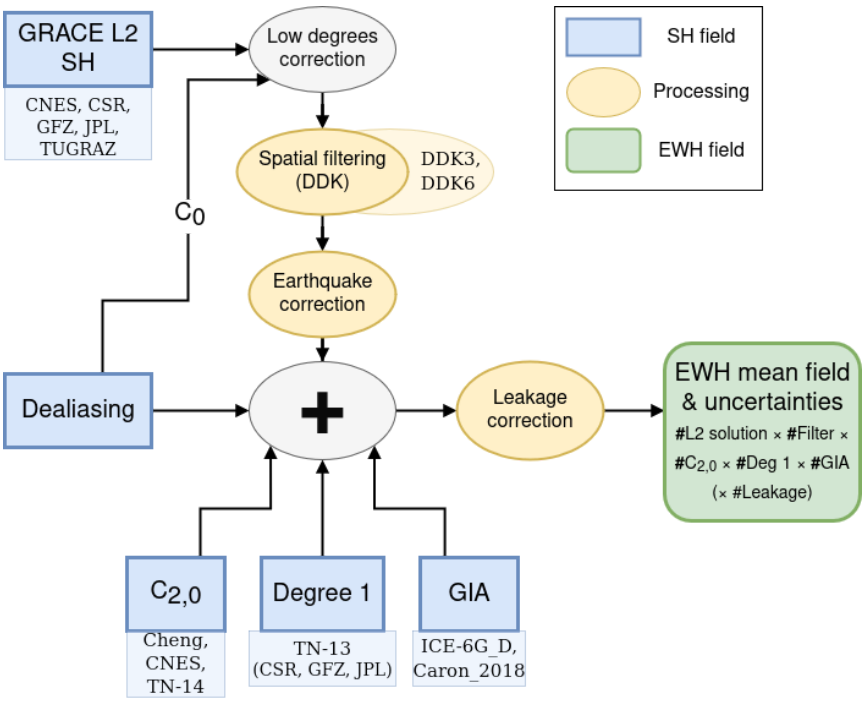

Figure 1: PANIS workflow indicating the main steps to convert GRACE/-FO Level-2 data into Level-3 SAGSA ensemble product. Blue boxes represent input data, yellow boxes indicate processing steps, and the green box shows the final ensemble solution. From (Lecomte et al., 2025).

1.3. Document structure

The structure of this document is as follows:

- **Section 2 – Input Data:** Describes all datasets and parameters required by PANIS, including their sources, formats, and any preprocessing steps necessary before they are used in the algorithm.
- **Section 3 – Output Data:** Details the products generated by PANIS, including their structure, format, and content, as well as any derived quantities or metadata provided alongside the main results.
- **Section 4 – Algorithm Description:** Provides a comprehensive explanation of the PANIS processing workflow, covering the methodology, sequence of operations, and any model corrections applied to transform the input data into the final output products.

1.4. Related documents

1.4.1. Bibliography

Bettadpur, S. (2007). *Level-2 gravity field product user handbook*. The GRACE Project (Jet Propulsion Laboratory, Pasadena, CA, 2003). https://archive.podaac.earthdata.nasa.gov/podaac-ops-cumulus-docs/grace/open/docs/L2-UserHandbook_v4.0.pdf

Blazquez, A., Meyssignac, B., Lemoine, J., Berthier, E., Ribes, A., & Cazenave, A. (2018). Exploring the uncertainty in GRACE estimates of the mass redistributions at the Earth surface : Implications for the global water and sea level budgets. *Geophysical Journal International*, *215*(1), 415‑430. https://doi.org/10.1093/gji/ggy293

Caron, L., Ivins, E. R., Larour, E., Adhikari, S., Nilsson, J., & Blewitt, G. (2018). GIA Model Statistics for GRACE Hydrology, Cryosphere, and Ocean Science. *Geophysical Research Letters*, *45*(5), 2203‑2212. https://doi.org/10.1002/2017GL076644

Carrère, L., & Lyard, F. (2003). Modeling the barotropic response of the global ocean to atmospheric wind and pressure forcing—Comparisons with observations. *Geophysical Research Letters*, *30*(6), 1275. https://doi.org/10.1029/2002GL016473

Chen, J., Cazenave, A., Dahle, C., Llovel, W., Panet, I., Pfeffer, J., & Moreira, L. (2022). Applications and Challenges of GRACE and GRACE Follow-On Satellite Gravimetry. *Surveys in Geophysics*, *43*(1), 305‑345. https://doi.org/10.1007/s10712-021-09685-x

Chen, J., Tapley, B., Seo, K.-W., Wilson, C., & Ries, J. (2019). Improved Quantification of Global Mean Ocean Mass

Change Using GRACE Satellite Gravimetry Measurements. *Geophysical Research Letters*, *46*(23), 13984‑13991. https://doi.org/10.1029/2019GL085519

Cheng, M. K., Ries, J. C., & Tapley, B. D. (2013). Geocenter Variations from Analysis of SLR Data. In Z. Altamimi & X. Collilieux (Éds.), *Reference Frames for Applications in Geosciences* (p. 19‑25). Springer. https://doi.org/10.1007/978-3-642-32998-2_4

Dahle, C., Flechtner, F., Murböck, M., Michalak, G., Neumayer, H., Abrykosov, O., Reinhold, A., & König, R. (2018). *GRACE Geopotential GSM Coefficients GFZ RL06* (Version 6.0, p. 3 Files) [Application/octet-stream,application/octet-stream,application/octet-stream]. GFZ Data Services. https://doi.org/10.5880/GFZ.GRACE_06_GSM

Dee, D. P., Uppala, S. M., Simmons, A. J., Berrisford, P., Poli, P., Kobayashi, S., Andrae, U., Balmaseda, M. A., Balsamo, G., Bauer, P., Bechtold, P., Beljaars, A. C. M., Van De Berg, L., Bidlot, J., Bormann, N., Delsol, C., Dragani, R., Fuentes, M., Geer, A. J., … Vitart, F. (2011). The ERA‑Interim reanalysis : Configuration and performance of the data assimilation system. *Quarterly Journal of the Royal Meteorological Society*, *137*(656), 553‑597. https://doi.org/10.1002/qj.828

Dobslaw, H., Bergmann-Wolf, I., Dill, R., Poropat, L., Thomas, M., Dahle, C., Esselborn, S., König, R., & Flechtner, F. (2017). A new high-resolution model of non-tidal atmosphere and ocean mass variability for de-aliasing of satellite gravity observations : AOD1B RL06. *Geophysical Journal International*, *211*(1), 263‑269. https://doi.org/10.1093/gji/ggx302

Gegout, P. (2012). Reference Loading Love Numbers. *Session G2.1, poster n°XL72*. EGU General Assembly.

GRACE-FO. (2024). *GRACE-FO Level-2 Monthly Geopotential Spherical Harmonics JPL Release 6.3* [Jeu de données]. NASA Physical Oceanography Distributed Active Archive Center. https://doi.org/10.5067/GFL20-MJ063

Jäggi, A., Meyer, U., Lasser, M., Jenny, B., Lopez, T., Flechtner, F., Dahle, C., Förste, C., Mayer-Gürr, T., Kvas, A., Lemoine, J.-M., Bourgogne, S., Weigelt, M., & Groh, A. (2020). *International Combination Service for Time-Variable Gravity Fields (COST-G) : Start of Operational Phase and Future Perspectives*. Springer Berlin

Heidelberg. https://doi.org/10.1007/1345_2020_109

Kusche, J., Schmidt, R., Petrovic, S., & Rietbroek, R. (2009). Decorrelated GRACE time-variable gravity solutions by GFZ, and their validation using a hydrological model. *Journal of Geodesy*, *83*(10), 903‑913. https://doi.org/10.1007/s00190-009-0308-3

Kustowski, B., Ekström, G., & Dziewoński, A. M. (2008). Anisotropic shear‑wave velocity structure of the Earth's mantle : A global model. *Journal of Geophysical Research: Solid Earth*, *113*(B6), 2007JB005169. https://doi.org/10.1029/2007JB005169

Kvas, A., Behzadpour, S., Ellmer, M., Klinger, B., Strasser, S., Zehentner, N., & Mayer‑Gürr, T. (2019). ITSG‑Grace2018 : Overview and Evaluation of a New GRACE‑Only Gravity Field Time Series. *Journal of Geophysical Research: Solid Earth*, *124*(8), 9332‑9344. https://doi.org/10.1029/2019JB017415

Landerer, F. W., Flechtner, F. M., Save, H., Webb, F. H., Bandikova, T., Bertiger, W. I., Bettadpur, S. V., Byun, S. H., Dahle, C., Dobslaw, H., Fahnestock, E., Harvey, N., Kang, Z., Kruizinga, G. L. H., Loomis, B. D., McCullough, C., Murböck, M., Nagel, P., Paik, M., … Yuan, D.-N. (2020). Extending the Global Mass Change Data Record : GRACE Follow-On Instrument and Science Data Performance. *Geophysical Research Letters*, *47*(12), e2020GL088306. https://doi.org/10.1029/2020GL088306

Lecomte, H., Blazquez, A., fourest, sebastien, meyssignac, benoit, pfeffer, julia, boughanemi, alexandre, & pellereau, eric. (2025). Leakage Corrections for GRACE Level-3 Solutions and Associated Induced Uncertainties. *IAG Proceedings 2025*.

Lemoine, J., & Reinquin, F. (2017). Processing of SLR observations at CNES. *Newsletter EGSIEM*, 3.

Lemoine, J.-M., & Bourgogne, S. (2020). *RL05 monthly and 10-day gravity field solutions from CNES/GRGS* (Nos. GSTM2020-51). GSTM2020. Copernicus Meetings. https://doi.org/10.5194/gstm2020-51

Loomis, B. D., Rachlin, K. E., & Luthcke, S. B. (2019). Improved Earth Oblateness Rate Reveals Increased Ice Sheet Losses and Mass-Driven Sea Level Rise. *Geophysical Research Letters*, *46*(12), 6910‑6917. https://doi.org/10.1029/2019GL082929

Martín‑Español, A., Zammit‑Mangion, A., Clarke, P. J., Flament, T., Helm, V., King, M. A., Luthcke, S. B., Petrie, E.,

Rémy, F., Schön, N., Wouters, B., & Bamber, J. L. (2016). Spatial and temporal Antarctic Ice Sheet mass trends, glacio‐isostatic adjustment, and surface processes from a joint inversion of satellite altimeter, gravity, and GPS data. *Journal of Geophysical Research: Earth Surface*, *121*(2), 182‐200. https://doi.org/10.1002/2015JF003550

Mayer-Gürr, T., Behzadpur, S., Ellmer, M., Kvas, A., Klinger, B., Strasser, S., & Zehentner, N. (2018). *ITSG-Grace2018—Monthly, Daily and Static Gravity Field Solutions from GRACE* (p. 4 Files) [Application/octet-stream,application/octet-stream,application/octet-stream,application/octet-stream]. GFZ Data Services. https://doi.org/10.5880/ICGEM.2018.003

NASA/JPL. (2023). *GRACE-FO Level-2 Monthly Geopotential Spherical Harmonics CSR Release 6.2 (RL06.2)* [Jeu de données]. NASA Physical Oceanography Distributed Active Archive Center. https://doi.org/10.5067/GFL20-MC062

Peltier, W. R., Argus, D. F., & Drummond, R. (2018). Comment on "An Assessment of the ICE-6G_C (VM5a) Glacial Isostatic Adjustment Model" by Purcell et al. *Journal of Geophysical Research: Solid Earth*, *123*(2), 2019‐2028. https://doi.org/10.1002/2016JB013844

Sun, Y., Riva, R., & Ditmar, P. (2016). Optimizing estimates of annual variations and trends in geocenter motion and J2 from a combination of GRACE data and geophysical models. *Journal of Geophysical Research: Solid Earth*, *121*(11), 8352‐8370. https://doi.org/10.1002/2016JB013073

Swenson, S., Chambers, D., & Wahr, J. (2008). Estimating geocenter variations from a combination of GRACE and ocean model output. *Journal of Geophysical Research: Solid Earth*, *113*(B8). https://doi.org/10.1029/2007JB005338

Tapley, B. D., Bettadpur, S., Ries, J. C., Thompson, P. F., & Watkins, M. M. (2004). GRACE Measurements of Mass Variability in the Earth System. *Science*, *305*(5683), 503‐505. https://doi.org/10.1126/science.1099192

Tapley, B. D., Watkins, M. M., Flechtner, F., Reigber, C., Bettadpur, S., Rodell, M., Sasgen, I., Famiglietti, J. S., Landerer, F. W., Chambers, D. P., Reager, J. T., Gardner, A. S., Save, H., Ivins, E. R., Swenson, S. C., Boening, C., Dahle, C., Wiese, D. N., Dobslaw, H., … Velicogna, I. (2019). Contributions of GRACE to understanding

climate change. *Nature Climate Change*, *9*(5), 358-369. https://doi.org/10.1038/s41558-019-0456-2

Yuan, D. (2019). GRACE Follow-On level-2 gravity field product user handbook. *Jet Propulsion Laboratory, JPL D-103922*.

1.4.2. Accronyms

Acronym	Description
AIUB	Astronomical Institute of the University of Bern
ATBD	Algorithm Theoretical Basis Document
CM	Center of mass
CNES	Centre National d'Études Spatiales
COST-G	Combination Service for Time-variable Gravity fields
CSR	Center for Space Research
DDK	Decorrelation and Denoising Kernel
DEM	Digital Elevation Model
ECMWF	European Centre for Medium-Range Weather Forecasts
EWH	Equivalent Water Height
GFZ	Geoforschungszentrum
GIA	Glacial isostatic adjustment
GPS	Global Positioning System
GRACE	Gravity Recovery And Climate Experiment
GRACE-FO	Gravity Recovery And Climate Experiment Follow-On
ITSG	Institute of Geodesy at Graz University of Technology
JPL	Jet Propulsion Laboratory
KBR	K-Band Ranging
L1B	Level 1B
L2A	Level 2A
L2B	Level 2B
L3	Level 3
L4	Level 4
LEGOS	Laboratoire d'Études en Géophysique et Océanographie Spatiales
LIA	Little Ice Age

LLN	Load Love Number
LRI	Laser Ranging Interferometer
NASA	National Aeronautics and Space Administration
NWP	Numerical Weather Production
PUM	Product User Manual
SAGSA	Service d'Activités en Gravimétrie Spatiale et Applications
SH	Spherical Harmonics
SLR	Satellite Laser Ranging
TUGRAZ	Technische Universität Graz
TWS	Terrestrial Water Storage

Table 1. List of abbreviations and acronyms

2. PANIS input data

2.1. Overview

In this section, we describe all external data used as input to the PANIS processing algorithm. Outputs generated internally by the algorithm that later serve as intermediate inputs are not discussed here; these are detailed in subsequent sections. PANIS relies on two principal categories of input data:

- Stokes coefficients, used to compute the various required spherical harmonic products (including GRACE Level-2 (L2) solutions, low-degree harmonic solutions, dealiasing fields, and GIA models).
- Spatial grids, used to apply corrections throughout the processing chain (including earthquake corrections, and the geomask grid).

The format, spatial resolution, and temporal sampling of all input datasets are described in the following subsections, along with an assessment of their limitations and a discussion of possible improvements for future versions of the algorithm. To determine which input with which parameters will be used for the combination, PANIS uses a configuration file in YAML format. This file orchestrates the processes applied to L2 solutions, which we describe in the following section.

2.2. Configuration yaml file

The yaml configuration file is where all the relevant information regarding the inputs, outputs and paths are stored. This file will first determine the name of the ensemble and the folder for all outputs of the chain (the folder will be created if not already existing). This file must contain the following fields:

- The **description** field containing the version and name of the ensemble,
- the **parameters** field containing the paths for the input and output of the chain, the flags for the writing of the diagnostics figures and files, and the chunk dimensions for the computations (used with xarray),
- the **time** field in which the period for the computation of the averages for the mean gravity field, GIA correction, … is computed,
- the fields for each input data: **dealiasing**, **processing_centers**, **C20**, **GIA**, **DEG1**, **filter**, **apriori**, **earthquakes**, **leakage**. These fields will have the paths to the folders where the data are stored, and when necessary the flags for their applications (e.g. the apriori flag). In order to add or remove data from the ensemble the user is invited to delete/comment the relevant fields or add new ones.

An example of yaml configuration is shown in Figure 2.

```yaml
description:
  version: 'V2.1'
  name: 'GRACE_ensemble_L3_V2.1'

parameters:
  input:
    path: '/work/scratch/data/boughaa/ensemble_V206/inputs/'
  output:
    path: '/work/scratch/data/boughaa/ensemble_V2.1'
  write_intermediate_files: True
  write_intermediate_diags: True
  write_final_diags: True
  chunks_size:
    time: 5
    product_center: 5
    product_filter: 2
    product_leakage: 1
    product_GIA: 2
    product: 1
    product_geocenter: 3
    latitude: 180
    longitude: 360

time:
  # Used to compute the mean gravity field
  period: ['2005-01','2014-12']

geomask:
  path: 'geomask/legos/GEO_mask_1deg_20231005.nc'


dealiasing:
  GAA:
    GFZ:
      path: 'L2_products/dealiasing/GFZ/GAA'
    CNES:
      path: 'L2_products/dealiasing/CNES/GAA.old'
```

```yaml
GIA:
  ICE6GD:
    path: 'GIA/ice6gd_2017/jgrb52450-sup-0003-data_s3.txt'
  Caron_2018:
    path: 'GIA/caron2018/expStokes_GIA.txt'

DEG1:
  Sun_CSR:
    path: 'geocenter/2025_Septembre_geocenter.nc'
  Sun_GFZ:
    path: 'geocenter/2025_Septembre_geocenter.nc'
  Sun_JPL:
    path: 'geocenter/2025_Septembre_geocenter.nc'


filter:
  DDK6:
    level: 6
  DDK3:
    level: 3

apriori:
    path: 'apriori/apriori_2025_janvier'
    flag_apply: False

earthquakes:
  Earthq0:
    path: 'earthquakes/usgs/list_earthquake_usgs.nc'
    selection: [1, 3, 5, 10, 11, 12, 13, 17]
    mode: 'direct'

leakage:
  AllContinents:
    correction_distance: 300
```

Figure 2: Example of the content of a PANIS yaml configuration file, here for the V2.1 of the L3 ensemble.

2.3. Level-2 GRACE/-FO geopotential solutions

2.3.1. Overview of L2 GRACE/-FO solutions

The GRACE and GRACE-FO Level-2 (L2) solutions provide monthly estimates of variations in the Earth's gravity potential, expressed in dimensionless spherical harmonic coefficients (Stokes coefficients C_{lm}, S_{lm}) that can be converted into physical units (equivalent water heights, gravity or geoid heights). L2 GRACE/-FO data represent geopotential anomalies relative to a set of background models that typically include:

- a static geoid model,
- solid Earth tides, ocean tides, solid and ocean pole tides, and atmospheric tides,
- non-tidal atmospheric and oceanic mass variations, and
- relativistic corrections.

All centers process the same L1B measurements including the intersatellite range and range rates measured by the K-Band Range (KBR) or Laser Range Interferometry (LRI), the range and phase measurements of each satellite from the GPS constellation, the accelerometers or transplant non-gravitational acceleration and the star trackers attitude data. The CNES centre also uses the satellite laser ranging (SLR) data. Because background models and inversion strategies differ across analysis centers, using L2 solutions from multiple centers allows us to assess uncertainties linked to these processing choices. The specific choices made by each center can be accessed in their respective documentation.

In this study, we use L2 solutions from five analysis centers:

- the CNES-SAGSA RL05 (J.-M. Lemoine & Bourgogne, 2020),
- the NASA Jet Propulsion Laboratory (JPL) RL06 2019 (Yuan, 2019) ,
- the TUGRAZ ITSG GRACE2018 (Mayer-Gürr et al., 2018),
- the GFZ RL06 (Dahle et al., 2018),
- the CSR RL06 (Yuan, 2019).

2.3.2. Format of the data

The L2 solutions are obtained in GRCOF2 files, corresponding to each monthly solution, separated in two parts: a header regarding the solution and 10 columns with the data. The header contains varying degrees of information regarding the data, depending on the providing center. The columns represent, in order:

- a keyword indicating that the line contains data,
- the harmonic degree,
- the associated order,
- the corresponding cosine coefficient,
- the corresponding sine coefficient,
- the standard deviation of the cosine coefficient,
- the standard deviation of the sine coefficient,
- the date of the first acquisition of the month,
- the date of the last acquisition of the month,
- a four letter indicator of whether the normalization is applicable (y) or not (n).

The file format is described in detail in the Level-2 Gravity Field Product User Handbook (Bettadpur, 2007). The maximum harmonic degree of each solution is 96, except for the CNES RL05 at 90.

2.3.3. Limitations

The ensemble approach enables exploration of uncertainties arising from differences in background models and inversion strategies (e.g., parameterizations, constraints). However, biases or errors shared across all analysis centers remain undetectable within this framework. When common processing strategies are widely adopted, any errors embedded in these shared methods cannot be evaluated through ensemble comparison.

The same instrumental uncertainties in the Level-1B (L1B) data affect all centers, yet information about the uncertainty is treated differently during inversion. Currently, ITSG is among the few centers that explicitly represent the statistical behavior of L1B instrumental uncertainties through variance–covariance matrices. Other centers have relied on prescribed uncertainty values, though CSR, JPL, and GFZ plan to adopt a variance–covariance-based approach in the upcoming RL07 release. Early tests show that incorporating full variance–covariance information at the L1B level reduces noise and improves solution stability. Nevertheless, other updates—such as revisions to the L1B data, the dealiasing model, or the reference frame—also contribute to the overall solution quality.

Finally, the diversity of background models demands careful tracking of consistency between processing and post-processing corrections. For example, both pole-tide and GIA corrections substantially affect the C_{21} and S_{21} geopotential coefficients. These contributions must be removed in a complete and internally consistent manner to isolate the component of the signal related to water-mass redistribution. Additional effort is needed to ensure that the pole-tide corrections applied by each center are fully compatible with the GIA models used in the PANIS post-processing chain. This process is handled directly by the lenapy python package, more detail on this can be found here: https://lenapy.readthedocs.io/en/latest/_static/Mathematics_consideration_for_LENAPY.pdf.

2.4. Degree-1

2.4.1. Description

The twin GRACE and GRACE-FO satellites orbit about the Earth's center of mass (CM) and are therefore insensitive to geocenter motion. As a result, the Level-2 geopotential solutions do not contain the degree-1 Stokes coefficients, which must be added a posteriori to obtain a complete representation of mass redistribution within the Earth system.

In the PANIS processing chain, degree-1 Stokes coefficients are reconstructed following the method of Sun et al., (2016). This approach assumes that geocenter motion can be inferred from the redistribution of mass estimated by GRACE/GRACE-FO at degrees ≥ 2, supplemented by external constraints from SLR (for C_{20}) and ocean reanalyses. The resulting geocenter motion is then converted into degree-1 geopotential coefficients (C_{10}, C_{11}, S_{11}), providing the missing low-degree component of the mass field.

Uncertainties in the reconstructed degree-1 terms are assessed by using multiple realizations of mass redistribution at degrees ≥ 2. PANIS therefore produces three independent degree-1 time series, derived from the GRACE/GRACE-FO L2 solutions provided by JPL, GFZ, and CSR, respectively. Additional methodological details are provided in the GRACE Technical Notes TN13a, b and c, itself based on the methodologies described in Sun et al., 2016; Swenson et al., 2008.

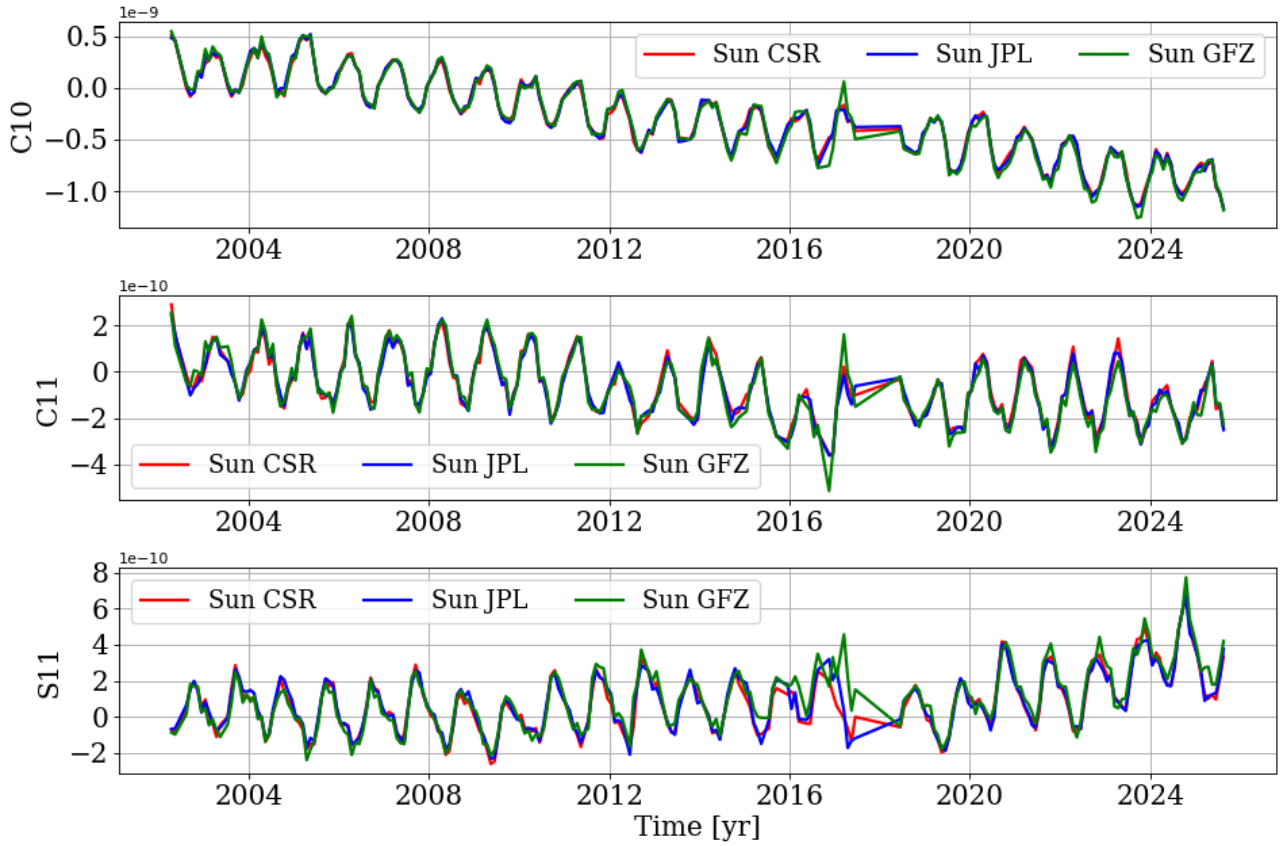

Figure 3: Time series of the three geocenter solutions used in the PANIS L3 ensemble.

2.4.2. Data Format

The degree 1 data come in a format similar to the L2 GRACE solutions described in the previous section, but without the four letter indicator. Each ensemble of 2 lines describes a set of C10/C11/S11 solutions for an observation period.

2.4.3. Limitation

The approach adopted here does not evaluate the error inherent to the method itself, but rather focuses on the dispersion of the mass distributions used to compute the geocenter motion and associated degree-1 coefficients. Ideally, the reconstruction would be performed internally using the same L2 data considered in the ensemble. In practice, however, the dispersion in the degree-1 estimate is small, and using three centers is likely sufficient.

Nie et al. (2025) further investigated the uncertainties associated with geocenter motion by considering GRACE/-FO L2 solutions, geophysical models, and SLR-derived geopotential solutions as alternative estimates of the Earth's system mass distribution. All three datasets yield consistent reconstructions of the degree-1 coefficients, although the SLR-based reconstructions exhibit higher noise levels due to their limited maximum resolution, which extends only up to degree 5.

Geocenter motion can also be directly inferred from SLR measurements, since satellites orbiting the Earth's center of mass are tracked by ground stations fixed to the crust, thereby establishing a direct connection between the center of mass and the network of tracking stations. In practice, however, SLR stations are referenced to the ITRF 2014, defined by a linear model whose origin follows the long-term center of mass as sensed by SLR. This approach leaves only

residual signals in the geocenter motions in SLR direct estimates. Consequently, the degree-1 field derived from this technique captures only the residual component relative to the ITRF, rather than the full degree-1 signal.

2.5. C20 and C30

2.5.1. Description

SLR monitors C_{20} by precisely tracking the orbital precession of satellites like LAGEOS, Starlette, Ajisaï, Stella and Lares. Changes in the nodal precession reflect changes in Earth's oblateness, which can be converted into temporal variations in C_{20}, revealing mass redistribution along the Earth's rotation axis. Since the C20 is not accurately observed by GRACE/-FO satellites, we use three SLR solutions provided by Cheng et al., (2013), J. Lemoine & Reinquin, (2017) and Loomis et al., (2019).

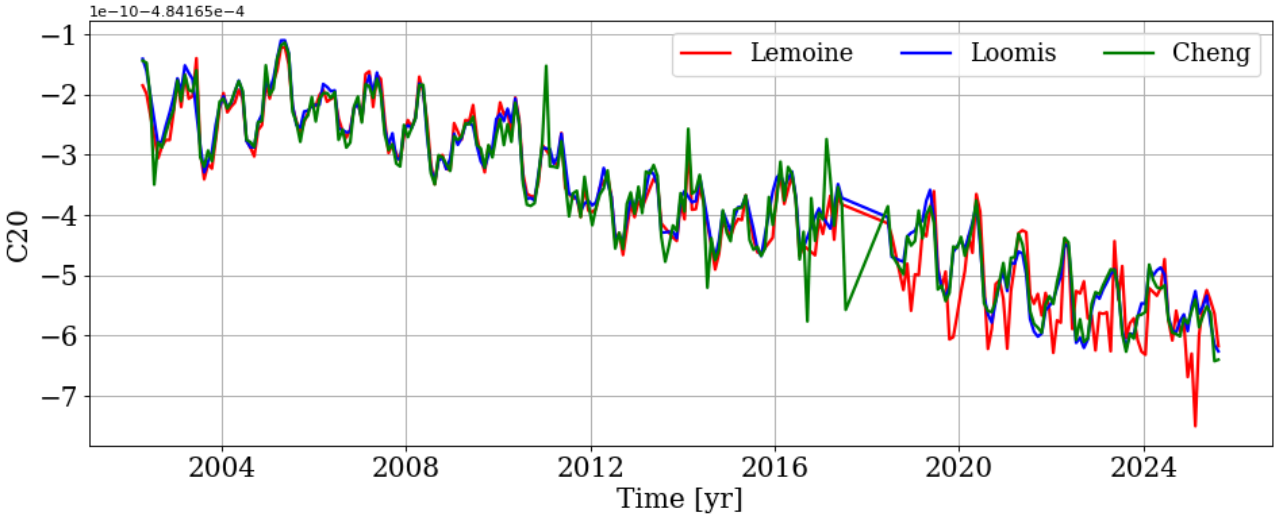

Figure 4: Time series of the C20 solutions used in the PANIS L3 ensemble.

We use only one C30 solution for the correction, which is obtained from the same source as one the C20 provider : Loomis et al., (2019). The C30 correction is provided starting March 2012, as before this period the solution for this coefficient is more robust and can be trusted.

2.5.2. Format of the data

The format of those solutions is again similar to that of the L2 solutions, without the four letter indicator.

2.5.3. Limitations

SLR-C_{20} is robust for detecting changes in Earth's oblateness associated with large-scale mass redistribution over decadal timescales. When using SLR-C_{20} in climate, sea-level, or ice-sheet studies, it is important to carefully consider systematic uncertainties, correlations with other spherical harmonics, and potential non-mass-related contributions (e.g., loading, GIA, atmosphere), which may not be fully accounted for in the solutions. Replacing GRACE C20 with SLR-C_{20} improves the stability at the global scale but does not eliminate all sources of uncertainty: noise, cross-term

correlations, and model dependencies persist. Moreover, while SLR-C_{20} provides a reliable long-term baseline, interannual variability should be interpreted with caution.

2.6. Ocean and atmosphere dealiasing

2.6.1. Description

The GRACE/-FO Atmosphere and Ocean De-aliasing datasets provide a priori information about the temporal variations in the Earth's gravity field caused by global mass variability in atmosphere and ocean. At Level-1B, AOD models are used to remove sub-monthly mass variations from the satellite measurements. At Level-2, they are used to restore physically meaningful signals—such as ocean circulation—and to maintain global mass conservation in the monthly gravity solutions.

The AOD1B RL06 (Dobslaw et al., 2018 and Dobslaw et al., 2019) model provided by GFZ is the current standard for both GRACE and GRACE-FO. It is based on analysis and forecast data out of the operational high-resolution global numerical weather prediction (NWP) model from the European Centre for Medium-Range Weather Forecasts (ECMWF) and ocean bottom pressure from an unconstrained simulation with the global ocean general circulation model MPIOM (Jungclaus et al., 2013) that is consistently forced with ECMWF atmospheric data. The CNES uses its own dealiasing model developped at OMP based on the ERA-interim reanalysis of ECMWF (60 model levels, every 3 hours) for the atmospheric part; and the TUGO barotropic model (Florent Lyard, LEGOS/CNRS) for the oceanic response to the ERA-interim pressure and wind forcing. The solid Earth response to the time-variable atmosphere & ocean potential has been taken into account through the use of the Love numbers (Gégout et al, 2009).

The Level-2 GAA, GAB, and GAC products provide monthly averaged Stokes coefficients for the atmospheric, oceanic, and combined atmosphere-plus-ocean contributions, respectively. The GAD grid, which is the GAC grid where the global average has been removed, is also computed later. OMP and GFZ products are available from the start of the GRACE mission (April 2002), although the OMP series ends in August 2017. The maximum spherical harmonic degrees are 90 for CNES and 180 for GFZ.

2.6.2. Format of the data

The GAA/B/C format is also very similar to that of the L2 GRACE solutions: a header regarding the solution and 10 columns with the data. The header contains varying degrees of information regarding the data depending on the providing center (OMP or GFZ). The columns represent, in order:

- a keyword indicating that the line contains data,
- the harmonic degree,
- the associated order,
- the corresponding cosine coefficient,
- the corresponding sine coefficient,
- the standard deviation of the cosine coefficient,
- the standard deviation of the sine coefficient,
- the date of the first acquisition of the month,
- the date of the last acquisition of the month,
- a four letter indicator of whether the coefficients are normalized (y) or not (n), and whether there is a stochastic a priori model for said coefficient (y) or not (n).

Users need to note that the coefficients from the two solutions are not sorted the same way. The OMP solution provides coefficients arranged in ascending degrees and orders (e.g. 20,21,22), while the GFZ solution arranges them in ascending orders (e.g. 10,20,30). When loading and sorting the coefficients, users need to be mindful of that.

2.6.3. Comments and limitations

When restoring atmospheric or oceanic de-aliasing fields, it is essential to ensure that the applied post-processing corrections are consistent with the background models used in generating the Level-2 solutions. This is particularly important for the tidal models: the de-aliasing fields represent departures from those background tides, so both must use harmonics treated in exactly the same way. Otherwise, certain periodic atmospheric or oceanic mass variations may be counted twice or omitted entirely.

Most analysis centers rely on the same non-tidal de-aliasing product—AOD1B RL06, developed by GFZ and described in Dobslaw et al. (2017). CNES is an exception: for the GRACE (2002–2016) period it uses atmospheric de-aliasing based on ERA-Interim and oceanic de-aliasing from the TUGO barotropic model. Since this creates limited model diversity within the ensemble, evaluating the influence of the de-aliasing choice on reconstructed Level-3 water-mass variability becomes challenging. A rigorous assessment would require controlled sensitivity tests in which identical processing chains are run with alternative de-aliasing models. Preliminary experiments underway within the SAGSA project point to a small but measurable impact of the de-aliasing model on the resulting gravity solutions.

A further limitation of the OMP products is their reduced maximum spherical-harmonic degree. As noted by Dobslaw et al. (2017), increasing the spatial resolution of GRACE/GRACE-FO gravity fields necessitates a corresponding increase in the resolution of the de-aliasing products. GFZ already provides AOD1B up to degree 180, offering more flexibility than the CNES fields, which currently extend only to degree 90.

2.7. GIA models

2.7.1. Description

The Glacial Isostatic Adjustment (GIA) is the response of the Earth’s system to past changes in ice and ocean loading, especially since the Last Glacial Maximum (~20,000 years ago). The redistribution of masses in the Earth’s interior produces long term changes in the Earth's geopotential, measured by the GRACE/-FO satellites. To extract signals due to present-day mass redistributions in the hydrosphere, ocean and cryosphere, GRACE and GRACE-FO data must be corrected for the ongoing deformations of the visco-elastic Earth due to the previous deglaciation. Two different GIA models are used here: the ICE6G_D model from Peltier et al. (2018) and Caron model from the mean estimated in Caron et al. (2018). No little ice age (LIA) correction is performed.

2.7.2. Format

Like the L2 GRACE solutions, the GIA models come in GRCOF2 files, with columns containing :

- a keyword indicating that the line contains data
- the harmonic degree
- the associated order
- the corresponding cosine coefficient

- the corresponding sine coefficient
- the standard deviation of the cosine coefficient
- the standard deviation of the sine coefficient
- the date of the model's construction

2.7.3. Comments and limitations

Only two GIA models are used, which limits our ability to fully assess the impact of the GIA model on the reconstructed water masses distributions. This limitation can be particularly important in regions where estimates of the GIA signal show substantial variability such as Antarctica (e.g. see Martín-Español et al. (2016).

Moreover, the representation of Earth's rheology in current GIA models may be insufficient to fully capture solid Earth deformations associated with past, recent, and present-day ice and ocean loading changes. Typically, GIA models adopt a Maxwell viscoelastic rheology with an upper mantle viscosity of 10^{21} Pa·s, and provide changes in the geopotential derived from the combination of coupled ice history and Earth rheology models. However, the ice histories used do not account for recent mass changes, such as those during the Little Ice Age. Conversely, deformations associated with present-day ice mass changes are often computed assuming a purely elastic Earth. This dual representation neglects the transient rheological response associated with recent or ongoing ice mass changes, leaving residual signals in the final products.

2.8. Earthquake data

2.8.1. Description

Earthquakes redistribute mass through the displacement of density interfaces—primarily the Earth's surface and the crustal base—and through density changes in rocks caused by sudden plate motion. GRACE and GRACE-FO have detected significant gravity changes for large events (Mw > 8), including shallow megathrust, strike-slip, and normal fault ruptures, as well as intermediate- and deep-focus earthquakes. Earthquakes produce abrupt co-seismic geopotential changes followed by post-seismic adjustments, which can continue for years to decades. To isolate contemporary surface water mass variations in GRACE/FO data, it is necessary to correct for earthquake-induced signals.

Correcting for earthquake effects requires knowledge of the earthquake's location, date, and an estimate of the affected zone. We use a USGS catalog (2004–late August 2015) of major events, which provides:

- The geographic location (longitude, latitude) and date of each event,
- The perimeter of the affected area, and,
- A relaxation time for modeling post-seismic adjustments.

This information allows us to construct time series to correct for earthquake-induced gravity variations. Users should note that some events are listed multiple times in the catalog (e.g., the 2004 Sumatra earthquake), so care is required to avoid overcorrection. Details of the correction methodology are provided in the section 4.7 of this document.

2.8.2. Comments and limitations

Currently, only the largest earthquakes (e.g., the 2004 Sumatra event) are considered in the corrections, as these are the only events detectable given the spatial resolution and accuracy of the available GRACE/-FO solutions. Future gravimetry missions with higher spatial resolution may allow detection of smaller earthquakes, which would then need to be accounted for. In the event of new major earthquakes (Mw > 8), corresponding corrections will be implemented in PANIS.

2.9. Auxiliary data

2.9.1. DDK filter parameterization

The DDK filter is a spectral decorrelation and smoothing method specifically designed to mitigate GRACE/-FO north–south correlated noise, balancing noise reduction with signal preservation (Kusche et al., 2009). The decorrelation step (the "D" part) targets characteristic north–south stripes by fitting and removing polynomials along lines of longitude in the spherical harmonic domain. The smoothing component attenuates high-degree harmonics dominated by noise while preserving large-scale geophysical signals. The design of the filter—including the choice of polynomial order and smoothing radius—is guided by typical error patterns in GRACE solutions.

These error patterns are represented in the NetCDF file ddk_normals.nc, which stores the filter coefficients and the normal-system approximation used to compute weights for each spherical harmonic coefficient. The file includes arrays defining the degree/order-dependent scale factors and metadata describing the filter configuration, allowing consistent application across multiple monthly solutions. ddk_normals.nc does not contain GRACE solution data itself, nor full covariance matrices; it provides pre-computed filter weights derived from representative GRACE error statistics, enabling efficient and consistent noise mitigation across the dataset.

Currently, only DDK filters of order 3 and 6 are used to generate the ensemble of filtered solutions. Using additional filter orders would increase ensemble size and memory requirements for both storage and computation.

2.9.2. Geomask data

The Geomask dataset from LEGOS (Université de Toulouse: CNES, CNRS, IRD, UPS) provides a global 1°×1° grid in which each cell carries Boolean descriptors characterizing its surface type. The dataset identifies continents, oceans, islands, basins, lakes, glaciers, and ice caps, and includes auxiliary geophysical attributes such as land elevation, distance to the coast, and cell surface area. All information is compiled in a NetCDF file containing the next variables expressed in regular grid of 1 degree latitude and longitude:

- cell surface area,
- land and ocean masks,
- land–ocean fraction,
- elevation from ETOPO and associated variability within the cell,
- coast-distance fields for oceanic cells,
- masks for major drainage basins,
- masks for small (<1 Mkm²) and large (>1 Mkm²) islands,
- masks for endorheic lakes,
- glacier masks,
- Antarctic basin masks.

Comments and limitations

Several limitations arise from the construction and resolution of this a priori model.

- The smallest lakes are neglected, an assumption appropriate for the current spatial resolution of GRACE/-FO but likely insufficient for future missions with higher maximum harmonic degree; additional lakes and river systems may need to be included.
- The 1° resolution inherently produces grid cells that overlap multiple surface types (e.g., coastal cells that include land, ocean, and lake surfaces). The boolean nature of the geomask can introduce errors in processes sensitive to surface extent, such as basin-integrated volume changes.

2.9.3. Love numbers

Elastic load Love Numbers (LLNs) describe how the solid Earth instantaneously deforms under the weight of a surface mass load, such as water, ice, or atmospheric pressure. They are fundamental parameters in GRACE/-FO processing because the satellites sense both the gravity change caused by the load and the gravity change caused by the Earth's elastic response to that load.

Here we use the LLNs from Gegout, 2012, computed for a spherically symmetric non-rotating, elastic and isotropic Earth model. Here the Earth model (i.e. 1D density and rigidity profiles) used is REF from Kustowski et al., 2008. The file contains a single column with only the values of the LLNs k', from degree 0 to 1024. It does not have any header or a second column with the corresponding degrees. The same format must also be used for any additional LLNs, regardless of the maximum degree computed. Users must be careful when changing the Love Numbers file, as the first value is expected to be for the degree 0.

While elastic load Love numbers are extensively employed to convert geopotential variations into surface mass changes in GRACE processing, comprehensive documentation detailing their theoretical basis, derivation, and implementation is missing. The overall method is described in Gegout, 2012.

3. PANIS Outputs

3.1. Main output

The primary output of the PANIS processing chain is a NetCDF file containing the ensemble of monthly gridded surface mass anomalies, expressed in equivalent water height (EWH). As of version 2.1, the ensemble can include up to 240 time series, depending on the combination of corrections applied to the GRACE monthly solutions.

The NetCDF file contains the following information:

- **Ensemble dimensions** reflecting the different processing choices applied:
    - `product_center` – the GRACE product center (e.g., CNES, GFZ, ITSG, JPL, CSR),

  - `product_filter` – applied decorrelation/smoothing filter(s) (e.g. DDK3, DDK6),
  - `product_earthquake` – earthquake correction applied,
  - `product_GIA` – GIA model applied (e.g. Caron, Peltier),
  - `product_leakage` – leakage correction applied,
  - `product_C20` – C20 solution applied (e.g. Loomis, Lemoine, Chen),
  - `product_geocenter` – geocenter solution applied (e.g. TN13a, b or c).
- **Spatial and temporal dimensions**:
  - `longitude` (360 values, 1° grid spacing),
  - `latitude` (180 values, 1° grid spacing),
  - `time` (238 monthly values starting from 2002-04-16 00:00:00, in hours).
- **Reference time** for the first monthly solution.
- **Water thickness time series** (`water_thickness`) for each combination of ensemble dimensions, representing surface mass anomalies in mEWH.
- **Boolean grids** defining land and ocean masks (`land_mask`).
- **Atmospheric water content grid** (`water_atmosphere_eq`) derived from GAA data, including metadata for Earth radius, gravitational constant, and maximum spherical harmonic degree.

All ensemble parameters, including the combination of corrections applied for each member, are stored as **variables in the NetCDF file** and are also documented in the YAML configuration file used for the run. The multi-dimensional structure of `water_thickness` allows users to extract a specific combination of corrections or generate an ensemble mean while retaining all applied processing options.

3.2. Intermediate grids

Specific correction grids can be accessed by enabling the option to save all raw grids used in the PANIS processing chain. These raw grids include each individual correction as well as the raw GRACE monthly solutions, some of which may not appear in the ensemble. The raw grids are stored in a NetCDF file, with a format similar to the ensemble file, and contain the following information:

- **Solution dimensions**, including:
  - GRACE product center,
  - Applied filter(s),

  - C20 solution(s),
  - GIA model(s),
  - Geocenter solution(s),
  - Leakage correction.

- **Spatial and temporal dimensions**: latitude, longitude, and time.
- **Time series** corresponding to each correction.

The raw grids file contains the same number of solutions as the ensemble. Additionally, separate files are generated for **leakage** and **earthquake corrections**:

- The **earthquake correction file** includes a correction for each combination of product center and filter used (up to 10 grids).
- The **leakage correction file** includes product centers, filters, GIA models, and earthquake corrections (up to 20 grids).

These grids are used for diagnostics if the user chooses to perform them. An additional NetCDF file containing the **ensemble mean** of the time series is also written. Users should note that generating and writing these raw grids can substantially increase the computation time of the processing chain.

3.3. Ensemble diagnostics

To verify the correct application of corrections, PANIS includes several diagnostic procedures that can be performed during processing. These diagnostics help users identify potential issues and evaluate the impact of each applied correction. To enable these diagnostics, the flags `write_intermediate_diags` and `write_final_diags` must be set to `True` in the YAML configuration file. The following sections describe the various types of diagnostics that can be generated during processing.

3.3.1. Initial diagnostics

The first set of diagnostics performed during the PANIS processing chain focuses on the **spherical harmonics data**, including the L2 GRACE products, C20 solutions, dealiasing products, and Geocenter solutions. These diagnostics provide the following information:

- **L2 products**: Time series of selected harmonic coefficients for each product center, compared with the Gravis correction, along with the spectral power of the L2 solutions before and after applying DDK filtering.
- **C20 solutions**: Time series of the C20 amplitude before and after processing for each solution.
- **Dealiasing products**: Time series for the GAC and GAD corrections, and a map showing the correction trend for GAD.

- **Geocenter solutions**: Time series of each degree-1 coefficient for all solutions.
- **GIA models**: Spectral power of the GIA corrections.

The specific figures and outputs generated depend on the parameters defined in the YAML configuration file.

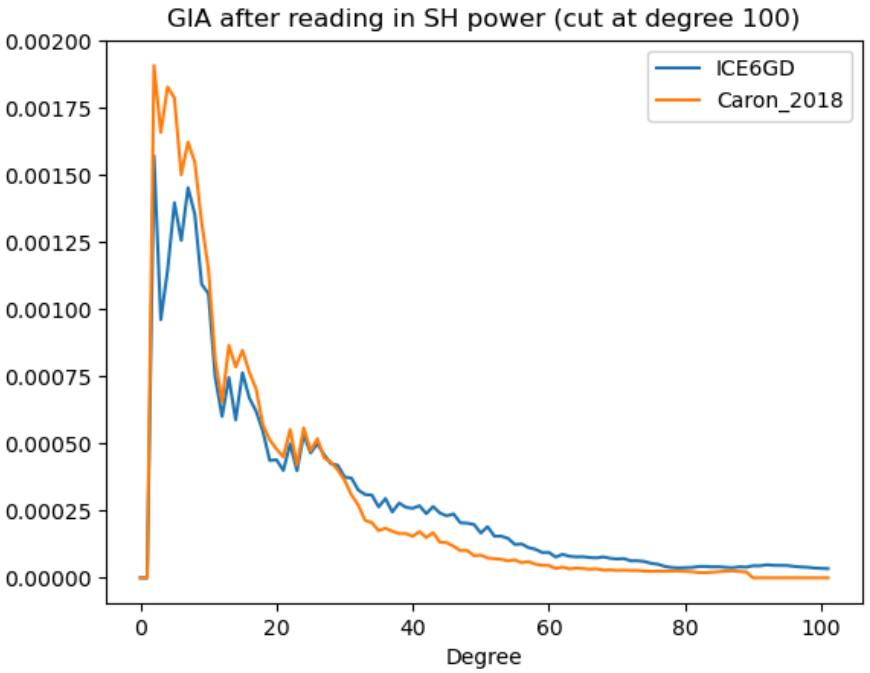

Figure 5: Example of the automated diagnostics figures from the ensemble, here showing the GIA spectral power.

3.3.2. Intermediate diagnostics

In the intermediate diagnostics, the raw grids described in the previous section are used to generate plots illustrating the **leakage** and **earthquake corrections**. Plots of adjustments applied to each correction for **mass conservation** are also produced. Diagnostics are performed for each GRACE product center and each relevant correction, as specified in the YAML configuration file.

The diagnostic figures include:

- **Earthquake corrections**:
    - Time series of the total mass change applied,
    - Time series of the mass adjustment applied for conservation of mass,
    - Plots of individual earthquake corrections, alongside the GRACE solutions before and after correction.

An example of correction is illustrated in section 4.7 where the earthquake correction method is described.

- **Leakage corrections**:
    - Map of areas affected by leakage,
    - Map showing the destination of the leakage correction,
    - Time series of the total mass correction applied.

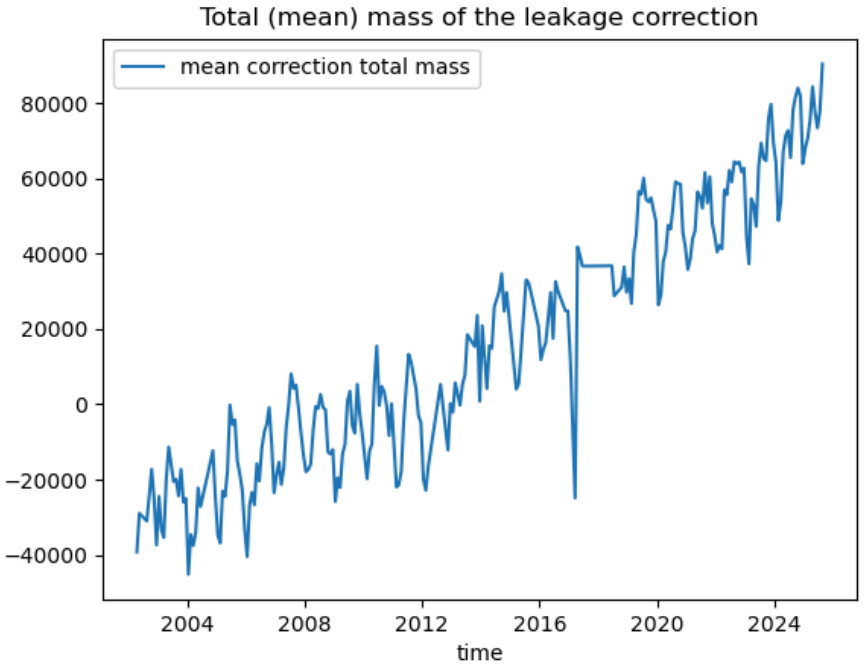

Figure 6: Example of diagnostic figure for the leakage correction.

3.3.3. Final diagnostics

At the end of the PANIS processing chain, a set of **final diagnostics** can be performed on the ensemble results. These diagnostics include a **statistical analysis** and a **global water budget study**.

The diagnostic figures include:

- **Statistical analysis**:
    - Maps of the **average annual water mass amplitude and phase** are produced, with uncertainties evaluated over the full ensemble period. Note that the **phase representation** can be further improved by using a **cyclic colormap** and converting the units from **degrees to months**.
    - Maps of the **average water mass trend** and associated uncertainties over the same period.
- **Global water budget**:

- Time series of the global water budget and each of its components, presented both before and after removal of the annual cycles.

- Plot of the **mass conservation correction** applied to the ensemble.

At the conclusion of the diagnostics, a file listing **missing months** in the ensemble—caused by poor-quality or noisy solutions—is generated. Because missing months can differ between centers, some months may be removed for other centers to maintain a **homogeneous ensemble**.

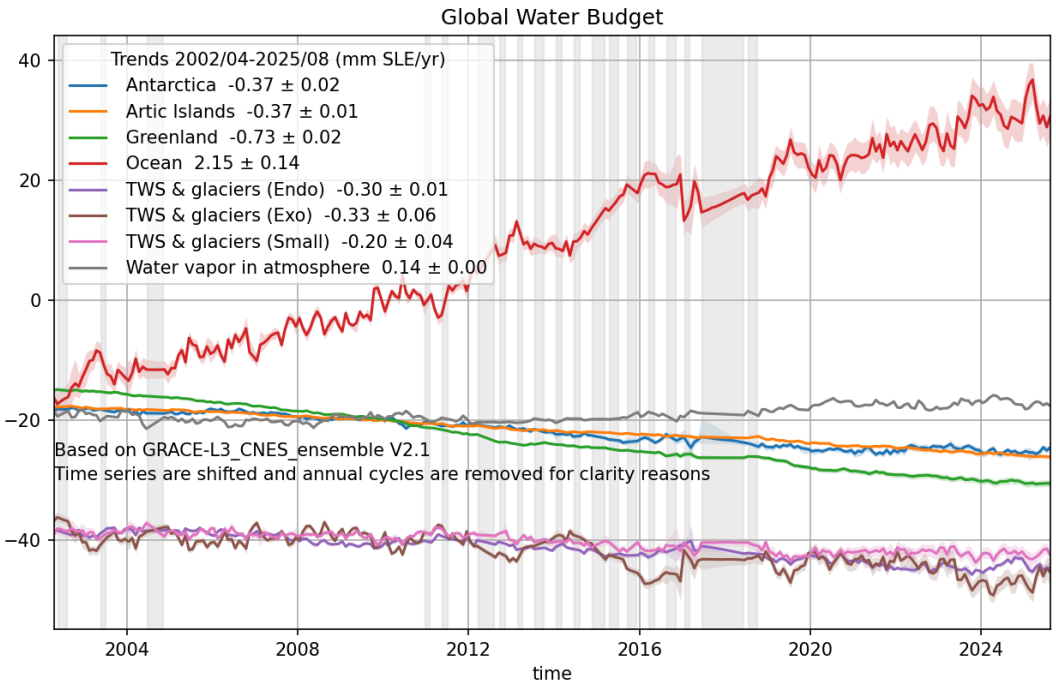

Figure 7: Example of the final diagnostics figures for the L3 ensemble, here the Global water budget after removal of the annual cycles.

4. PANIS processing algorithm

4.1. Overview

This section describes the processes used to convert the L2 GRACE geopotential solutions into L3 gridded surface mass anomaly maps. The spatial and temporal resolution of the resulting grids depends on the GRACE solution used and the set of corrections applied. All parameters for a PANIS run are specified in a YAML configuration file, which defines the list of corrections, their maximum harmonic degree, and the input and output paths for each dataset.

The GRACE solutions are available monthly up to degree 96, corresponding to a spatial resolution of approximately 300 km. The a priori model, earthquake, and GIA corrections are applied on 1°×1° grids, and the spherical harmonics

expansion of the monthly solutions is performed on the same grid. Some monthly solutions are missing or contain very noisy signals; these are excluded from the final L3 grids produced by PANIS.

Figure 8 provides an overview of the PANIS processing algorithm. All grids produced at each step are expressed in equivalent water height (EWH) to remain consistent with the GRACE solutions. The following subsections describe the algorithm in detail.

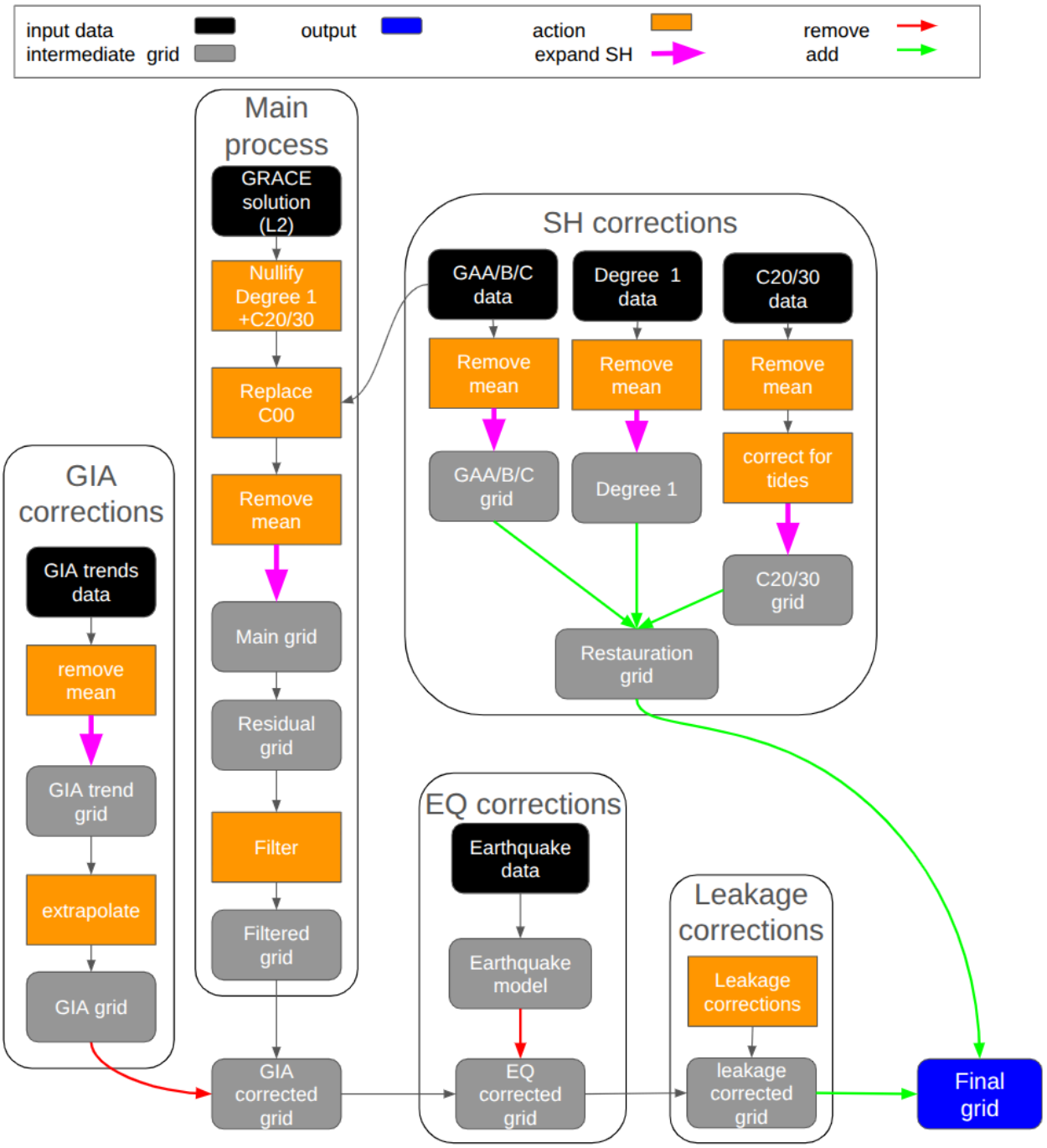

Figure 8: Overview of the PANIS processing algorithm. All intermediate grids (e.g. GIA, Degree 1 or C20) are computed with the same 1°x1° resolution, and are saved for further analysis during and after the processing.

4.2. Main assumptions

4.2.1. Spherical harmonic expansion

The **Stokes coefficients** are expanded assuming a **spherical Earth**, with the radius taken as the mean equatorial radius (~6378.136 km) (Wahr, 2018). In previous versions of PANIS, an equation accounting for Earth's ellipticity was used (Ditmar et al., 2018); in this version, we use the spherical Earth approximation allowing a more accurate conservation of mass. More details are provided in Section 4.4.

4.2.2. Elastic rheology

To convert geopotential anomalies into **gridded surface mass** anomalies, we assume **elastic load Love numbers** (Kl). Consequently, **non-elastic signals** associated with the deformation of the solid Earth are not accounted for and remain in the ensemble. These signals will therefore be interpreted as surface mass anomalies. This assumption is applied uniformly across all ensemble members, and is **not explored in the ensemble dispersion**.

4.2.3. GIA correction

The **GIA correction** is assumed to be **linear over time**, allowing extrapolation for each monthly solution. This assumption may be limited, particularly in regions with current-day ice melting, such as Antarctica and Greenland.

4.2.4. Post-seismic corrections

The **post-seismic signal** is not corrected. We assume that earthquake-related corrections consist of an instantaneous jump followed by an exponential decay. As the post-seismic trend is difficult to estimate and isolate from the ensemble signal, it remains in the output. Future versions of PANIS may include explicit post-seismic corrections.

4.2.5. Ensemble assumptions and limitations

The ensemble approach reflects only selected sources of uncertainty, such as the processing of L1B to L2 data, filtering, GIA, degree-1 and degree-2 corrections. Common sources of error, including assumptions on elastic Earth response and unmodeled geophysical signals, are not captured by the ensemble dispersion. Users should interpret ensemble uncertainties as representative of a subset of processing-related variations, not total geophysical or measurement uncertainty.

4.3. Reading tools

To handle the diverse input files, which vary in both header structure and data format, `readers.py` provides specialized functions that extract spherical harmonic coefficients in a consistent manner. These functions support a range of datasets, including C20 and low-degree coefficients from various sources, GIA harmonic coefficients from ICE6G_D and Caron et al., degree-1 solutions, and the Geomask data. Each function parses the file until the header

ends, then stores the coefficients in a dataset for combination with GRACE/-FO solutions or for generating correction grids during ensemble creation. Alternatively, users can load all coefficients from a pre-aggregated NetCDF file, which simplifies input handling; this option must be specified in the YAML configuration file.

4.4. Conversion of geopotential coefficients to surface water grids

The mathematical foundation of the PANIS software is based on LENAPY. The official documentation for LENAPY is available at: https://lenapy.readthedocs.io/en/, and the document detailing its mathematical foundations can be found here: https://lenapy.readthedocs.io/en/latest/_static/Mathematics_consideration_for_LENAPY.pdf .

To convert geopotential anomalies expressed as Stokes coefficients into gridded surface water mass anomalies, PANIS uses the formula from Wahr (1998), which projects the solution onto the sphere:

$$\Delta H_{\mathrm{w}}(\theta,\phi) = \frac{a}{3}\frac{\rho_{\mathrm{E}}}{\rho_{\mathrm{w}}}\sum_{l=1}^{L_{\max}}\sum_{m=-l}^{l}\frac{(2l+1)}{(1+k_l)}\Delta C_{lm}\bar{Y}_{lm}(\theta,\phi)$$

where:

- $\Delta H_W(\theta,\phi)$ is the equivalent water height at the latitude θ and longitude ϕ,
- a is the Earth radius,
- ρ_E is the average density of the Earth,
- ρ_w is the density of water,
- k_l is the elastic load Love Number for any harmonic degree l,
- $\bar{Y}_{lm}$ are the legendre polynomial function for any degree l and order m, and,
- ΔC_{lm} are the spherical harmonic coefficients of the solution.

The computation of the grids for each degree and order is parallelized using Dask and Xarray to accelerate the conversion.

The input for the expansion is a set of Stokes coefficients up to the harmonic degree required by the user. These coefficients are stored in GRCOF2 files (see Section 2). The maximum harmonic degree depends on the product (e.g., 96 for L2 GRACE solutions, 256 for GIA models) and user requirements, which are specified in the YAML configuration file. Other parameters for the expansion, such as grid boundaries or Legendre polynomial normalization, can also be set in the YAML file if the defaults do not meet user needs.

The output of the spherical harmonic expansion is a grid of the physical parameter corresponding to the Stokes coefficients. In PANIS, each grid represents a surface mass anomaly expressed in equivalent water height (EWH). By default, grids are 1°×1° with latitudes from -89.5° to 89.5° and longitudes from 0.5° to 359.5°, though these can be adjusted depending on user requirements.

Producing finer-resolution grids, and therefore ensembles, requires substantially more computational and storage resources. For example, in version V2.1 of the ensemble, generating 180 solutions on 1°×1° grids requires

approximately 21 GB of storage for the ensemble alone and around 3 hours of computation to produce the ensemble and all auxiliary files and figures. Reducing the grid spacing further will significantly increase both computation time and resource demands.

4.5. Filtering tools

The **filtering of the solutions** in PANIS is performed using functions from the `filter_ddk.py` script. Two main functions are employed for applying the DDK filter:

1. **Loading DDK coefficients**:

   The first function reads the DDK coefficients of the required order from the `ddk_normals.nc` file. Nine options are available:

   - Input `0` applies **no filtering**.
   - Inputs `1` to `8` apply DDK filters of increasing order, where `1` applies the **strongest filtering** and `8` the **weakest**.

   Currently, DDK filters are applicable only for solutions up to **degree and order 120**. Solutions with higher degrees would require an update to both the coefficient file and the code.

2. **Applying the DDK filter**:

   The second function applies the DDK filter to the solution by performing an element-wise multiplication of each spherical harmonic coefficient by its corresponding filter factor: $\hat{C}_{lm} = C_{lm} \cdot F_{lm}$,

   where :

   - $\hat{C}_{lm}$ is the filtered spherical harmonic coefficient,
   - C_{lm} is the spherical harmonic coefficient to filter, and,
   - F_{lm} is the filter applied.

The filter is obtained using the normal numbers found in the NetCDF file from the Panis resources folder, and are computed for each level of filtering such as: $F_{lm} = A_{lm}^{-1} \cdot N_{lm}$ where N_{lm} is the normal number for the degree l and order m, and $A_{lm}^{-1} = N_{lm} \cdot W_{lm}$ is the weighted normal number.

The weights depend on the DDK order and are set as the DDK scale to the power of 4, following Kusche et al., 2009. The scales used in PANIS are summarized in Table 2:

No filtering	DDK 1	DDK 2	DDK 3	DDK 4	DDK 5	DDK 6	DDK 7	DDK 8
0	1e14	1e13	1e12	5e11	1e11	5e10,	1e10	5e9

Table 2 : DDK filters scales used in Panis

It is possible to modify those scales by interacting directly with the DDK filtering function, but it is not recommended.

4.6. Leakage correction tools

The leakage correction tool mitigates leakage errors found in surface mass anomaly fields near the coastline. Leakage errors arise from the limited spatial resolution of the satellite configuration and from the inversion approach, which estimates the gravitational potential using a truncated set of spherical harmonic coefficients, often producing Gibbs-type oscillations. Leakage errors are propagated during the filtering step, which is necessary to mitigate the noise and extract statistically significant signals. Within PANIS, leakage errors are defined within a specified distance of the coastline as the deviation from the ocean basin average. Mass anomalies incorrectly mapped over the ocean are then reassigned to adjacent land areas using weights derived from land–ocean distance and surface cell area, ensuring strict mass conservation. The algorithm can be described in three main steps as follows.

1. **Generation of the leakage land and ocean masks**

The leakage ocean mask $\mathbf{M}_{OL}$ identifies ocean grid cells where leakage errors are to be removed. It is defined as:

$$\mathbf{M}_{OL} = \mathbf{M}_{ocean} \cap (\mathbf{d}_{coast} < D) \quad (1)$$

, where

- $\mathbf{M}_{ocean}$ is a boolean mask of all ocean grid cell described in the geomask file (section 2.9.2)
- $\mathbf{d}_{coast}$ is the distance from the coast, which is positive over the ocean and negative over land, as described in the geomask file
- D is the maximum distance from the coast where leakage errors can be identified. This distance is specified by the user in the yaml file as described in section 2.2.

The leakage land mask $\mathbf{M}_{LL}$ identifies land grid cells where leakage errors are to be added back. It is defined as:

$$\mathbf{M}_{LL} = \mathbf{M}_{land} \cap (-D \leq \mathbf{d}_{coast} < 0) \quad (2)$$

, where

- $\mathbf{M}_{land}$ is a boolean mask of all land grid cells described in the geomask file (section 2.9.2)

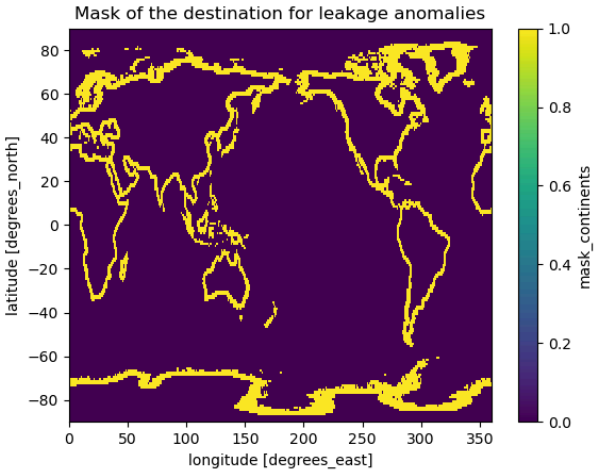

FigureFigure 9: Example of land leakage mask

2. **Computation of leakage errors**

Leakage errors are defined within the ocean leakage mask as the deviation of the surface mass anomalies from the ocean basin average:

$$\Delta_i = \sigma_i - \frac{\sum_{k \in \mathbf{M}_{basin}} \sigma_k \cdot a_k}{\sum_{k \in \mathbf{M}_{basin}} a_k}$$

Where:

- Δ_i is the leakage error at grid cell i within $\mathbf{M}_{\mathrm{OL}}$.
- σ_i is the surface mass anomaly (e.g., in equivalent water height) at grid cell i.
- $\mathbf{M}_{basin}$ is the mask of the ocean basin containing the cell i.
- σ_k is the surface mass anomaly at any cell k within $\mathbf{M}_{basin}$
- a_k is the surface area of grid cell k within $\mathbf{M}_{basin}$.

The fractional term represents the area-weighted average of the surface mass anomalies over the entire basin region. The division in basins is shown in Figure 10.

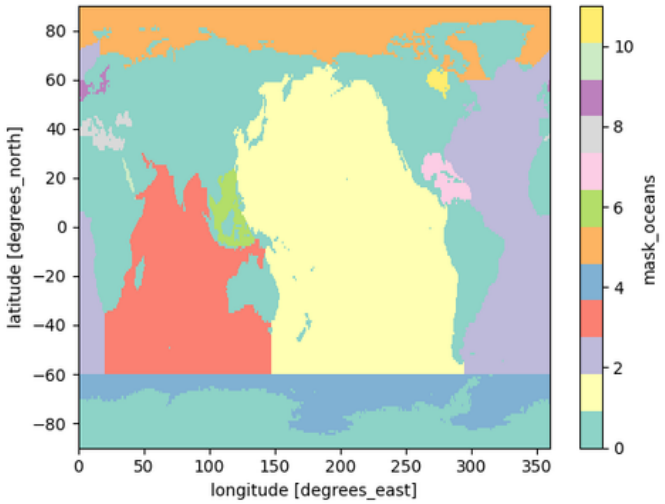

Figure 10: Mask of each ocean basin considered for the leakage correction. The continents are shown with the color corresponding to the value 0.

3. Reallocation of the leakage errors on land

The leakage error is redistributed from the ocean cells i in M_{OL} to the land cells j in M_{LL} using the weights w_{ij} derived from a normalized, inverse-distance weighting and a surface-area ratio, ensuring both proximity-based distribution and mass conservation.

$$w_{i,j} = \frac{1}{d_{i,j} \cdot \sum_{k \in \mathbf{M}_{LL}} \frac{1}{d_{i,k}}} \cdot \frac{a_i}{a_j} \tag{3}$$

where:

- $d_{i,j}$ is the distance between the ocean cell i and the land cell j
- $d_{i,k}$ is the distance between the ocean cell i and the land cell k

The corrected surface mass anomalies σ^L_j in land cell within $\mathbf{M}_{LL}$ can then be calculated as:

$$\sigma_j^L = \sigma_j + \sum_{i \in M_{OL}} \Delta_i w_{i,j} \tag{4}$$

where:

- σ_j is the uncorrected surface mass anomaly in land cell j

The corrected surface mass anomalies σ^L_i in ocean cell i within $\mathbf{M}_{OL}$ are simply calculated as the area weighted ocean basin average

$$\sigma_i^L = \frac{\sum_{k \in \mathbf{M}_{basin}} \sigma_k \cdot a_k}{\sum_{k \in \mathbf{M}_{basin}} a_k}$$

And the surface mass anomalies outside the leakage ocean and land mask cells are preserved without modification.

4.7. Earthquake correction tools

The earthquake correction in PANIS requires several user-specified inputs in the configuration file. The user must indicate which earthquakes are to be corrected, referencing the USGS NetCDF file described in Section 2.6. This file provides three essential elements for each earthquake:

1. **Location and exact date** (in decimal years),
2. **Impact distance**, which defines the area affected for the correction,
3. **Relaxation time**, describing the exponential decay of the post-seismic signal.

Additionally, the user can specify the **correction mode**. Two modes are available in PANIS v2.1:

- **Direct mode:** Fits the co-seismic jump and the immediate relaxation.
- **Post-trend mode:** Fits the jump, relaxation, and an additional linear post-seismic trend.

For version 2.1, only the jump and exponential relaxation are applied.

Correction procedure:

1. **Mask creation:** A boolean mask of the affected zone is generated using the impact distance from the USGS file.
2. **Co-seismic correction functions:** For each earthquake, two functions are computed to model the co-seismic response:
   - a Heavyside function to correct the jump at the exact time of the earthquake:

     $$H(t) := \begin{cases} 1 \times I, & t \geq t_0 \\ 0, & t < t_0 \end{cases}$$

     where t is the time and t_0 is the exact time of the earthquake. The amplitude I of the jump is obtained later by least squares.

   - an exponential decaying of the signal following immediately after the earthquake:

     $$D(t) := \begin{cases} I(1 - e^{\frac{-(t-t_0)}{\tau}}), & t \geq t_0 \\ 0, & t < t_0 \end{cases}$$

     where t is the time, t_0 is the exact time of the earthquake and τ is the relaxation time given by the usgs file.

- If the user chooses to apply also a correction for the post-seismic trend, a third function will also be computed for the linear correction:

$$L(t) := \begin{cases} (t - t_0) \times I, & t \geq t_0 \\ 0, & t < t_0 \end{cases}$$

3. **Amplitude estimation:** The amplitude of the co-seismic jump and the post-seismic relaxation is estimated separately for each GRACE solution center (e.g., CNES, JPL, CSR). For each affected location, the observed time series is fitted using a combination of functions representing the climatological signals (annual and semi-annual cycles, mean, and trend) along with the co-seismic jump and exponential relaxation. The fitting process determines the magnitude of the jump and decay that best explains the observed signal. These estimated amplitudes are then used to generate the correction time series for each earthquake and each solution, which are subsequently combined into grids for use in the ensemble.

An example of earthquake correction is shown in Figure 11. Once all the different corrections are computed they are then stored in a dataset to use for the combination of the ensemble.

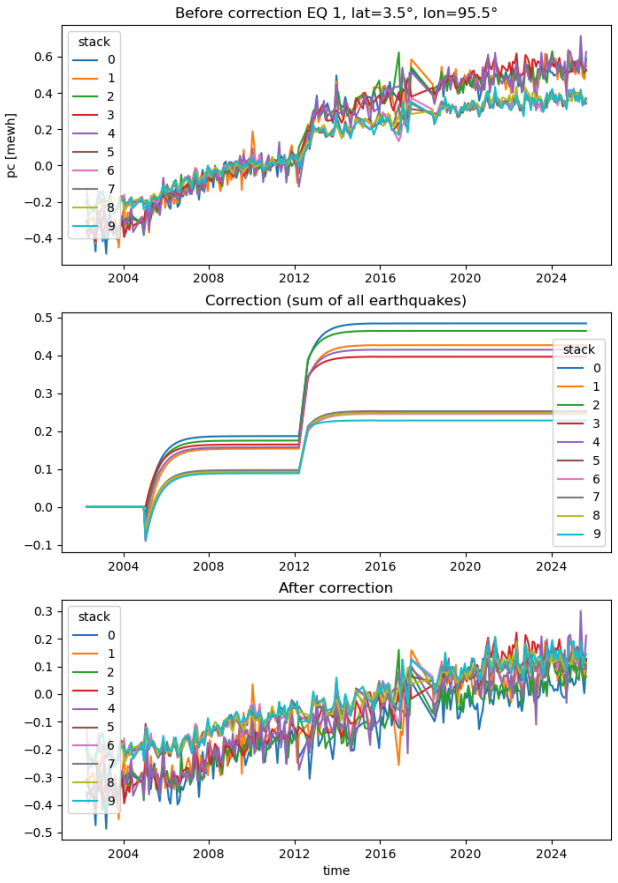

Figure 11: Example of time series correction for the Sumatra region. Each number represents a combination of a solution from any of the processing centers (CNES, CSR, …) and a DDK filter (order 3, 6, …). Here we have 10 numbers, representing 5 centers and two DDK filters.

4.8. Main process

This section describes the main procedure for generating the ensemble, including the sequence of combination steps performed during processing. The workflow begins by creating an output directory defined by the destination specified in the configuration YAML file. All products generated by the PANIS workflow are stored in this directory, including the ensemble output, the configuration file, and any diagnostic figures. Once the directory is initialized, the ensemble generation process proceeds as detailed in the following sections.

4.8.1. Raw grids computation

The first step in the main workflow is the generation of the initial grids used to construct the ensemble. This stage consists of several operations.

4.8.1.1. First Step

The dealiasing models are first loaded and stored in separate datasets. In the GAB dataset, the C00 coefficient is set to zero, and the mean dealiasing field over the user-specified period (defined in the YAML configuration file) is removed. A separate dataset containing the atmospheric C00 time series from the GAA product is also created for later use. Both sets (GAA and GAB) of dealiasing grids are then generated. When CNES RL05 solutions are included among the L2 products to be processed, an additional set of dealiasing grids is produced. In this set, the GAA and GAB models from GFZ are removed from the OMP dealiasing model—restricted to the GRACE period—and these grids are the ones used for the CNES solutions during the restoration of the dealiasing. This is done to ensure consistency with the other L2 solutions.

Next, the GAC grids are computed as the sum of the GAA and GAB grids, and the GAD grids are generated by applying an ocean mask to the GAC fields. The global GAD field, defined as the temporal mean of the GAD grids, is then computed and stored with the other datasets for later use during the combination step. If enabled by the user, a first set of diagnostic figures for the dealiasing products is produced at this stage. This completes the first step.

4.8.1.2. Second step

The second step involves computing the raw L2 grids using the L2 solutions together with the dealiasing datasets generated previously. All L2 solutions for all time steps are loaded, after which the atmospheric C00 time series is removed and all degree-1 coefficients are set to zero. For each center, the C20 coefficient is set to zero. All C30 coefficients are replaced with those from the TN14 low-degree SLR solution (Loomis et al., 2020). The mean field over the selected period is then removed, and, if requested by the user, the selected a priori model is subtracted from the harmonic coefficients.

At this point, DDK filtering is applied following the methodology described in Section 4.5. The filtering levels are specified in the YAML configuration file. By default, two filtering levels (DDK3 and DDK6) are applied, but additional levels may be included. The filtered solutions are then gridded and concatenated into a dataset.

If requested by the user, diagnostic figures are generated at this stage, as described in Section 3.

4.8.1.3. Third step

The third step is the generation of the GIA correction grids. The spherical harmonic coefficients for the two GIA models are loaded and converted to equivalent water height trend grids. These trend grids are then used to compute the GIA correction at each time step using the formulation:

$$GIA(t) = GIA_{trend} \times (t - t_0)$$

where t is the time and t_0 is the beginning date of the GRACE/-FO missions. The times series are then centered at the same time as the L2 solutions in order to properly remove the GIA signals. The correction for the two GIA models is then stored in a dataset, to be used to correct the gridded L2 solutions as $L2_{cor} = L2 - GIA$ later during the combination process.

4.8.1.4. Fourth step

The fourth and last step is the creation of the degree-1 and C20 grids. These two types of grids follow the exact process: the spherical harmonics are loaded into datasets, then the average over the selected period is removed and the coefficients are converted into grids.

All these grids are then concatenated into a single dataset to use later for the combination. This dataset can be saved as one of the outputs of the PANIS process if the user needs it.

4.8.2. Solid Earth corrections

The second stage of the main workflow removes the earthquake and GIA correction grids to the L2 grid series generated previously. The earthquake correction, described in section 4.7, does not change the number of solutions as at the moment a single correction is applied homogeneously to all ensemble members.

The Glacial Isostatic Adjustment (GIA) correction described in sections 2.7 and 4.8.1 is then applied. Unlike the earthquake correction, this step can increase the number of solutions because PANIS currently includes two GIA models. For example, in ensemble version 2.1, both models are applied, bringing the total number of solutions at this stage to 20.

4.8.3. Dealiasing restoration

The next step in the generation of the ensemble is the restoration of the dealiasing model. The GAD grids have been computed previously as described in section 4.8.1.1. Then, the global mean of the GAD grids is calculated at each time step and removed from the GAD grids. The GAD grids corrected from their global mean are added back to the L2 grids. This process ensures that the surface mass anomalies can be compared with sea level estimates from altimetry. The dealiasing restoration enables to add back the signal from the ocean circulation but not from the atmosphere. The atmosphere water content grids (GAA) are added in a separate array to the ensemble file afterward, after the end of the combination process.

4.8.4. Leakage correction

Next is the application of the leakage correction. As of version 2.1 of the ensemble only one correction method is employed, described in section 4.6. In future versions of PANIS more correction methods will be added. The correction is applied to all ensemble members homogeneously.

4.8.5. Final combination

The final step of the combination is to add back the low degrees grids generated previously to the filtered surface mass anomalies corrected for Solid Earth leakage corrected with dealiasing restored. At this step the solutions have been corrected for all the unwanted signals, and only the restoration of the low degrees remains. At this point the number of solutions will drastically increase, as the 20 corrected solutions will be combined with all the geocenters and C20 solutions. For example, for V2.1 the 20 corrected solutions are combined with the 3 geocenters and the 3 C20 solutions, to create the 180 solutions of the ensemble. At this point, if the user requires them, a series of diagnostic figures are generated concerning the total mass balance of the ensemble.

The combination process is summarized by the following equation (we remove the three dimensions θ, λ, t for simplicity):

$$\sigma_{L3}(i,j,k,l,m) = L\left[\sigma\left(F(j)\cdot\delta_{L2*}(i)\right) - \sigma_{EQ} - \sigma_{GIA}(k) + \sigma_{GAD*}\right] + \sigma_{C20}(l) + \sigma_{GEOC}(m)$$

where:

- $\sigma_{L3}(i,j,k,l,m)$ is the L3 grid generated with the combination,
- L is the leakage correction applied to the grids filtered, corrected for solid earth signals and with the dealiasing restored,
- $\delta_{L2*}(i)$ are the L2 spherical harmonic solutions, for which the degree 1 and C20 have been nullified and the GAA C00 has been removed,
- $F(j)$ is the DDK filter of order j applied to the spherical harmonic solutions corrected for the mass conservations and low degrees,
- $\sigma\left(F(j)\cdot\delta_{L2*}(i)\right)$ are the grids generated for the each filtered L2 solution,
- σ_{EQ} are the earthquake correction grids removed to the filtered L2 grids,
- $\sigma_{GIA}(k)$ are the GIA correction grids for any model k removed to the filtered L2 grids,
- σ_{GAD*} are the dealiasing restorations grids from which the global average GAD has been removed,
- $\sigma_{C20}(l)$ are the C20 grids computed for solution l, added back to the corrected grids
- $\sigma_{GEOC}(m)$ are the degree 1 grids computed for solution m, added back to the corrected grids.

Once all the solutions have been computed, the atmosphere water content grids are added to the dataset and it is then saved as a NetCDF file in the directory specified in the configuration file. The final set of diagnostic figures are then produced if required, as described in section 3.3.3. The final output of the PANIS chain, which is the ensemble average,is then generated and saved at the same location as the whole ensemble.

5. Uncertainties retrieval method

The methodology for deriving uncertainties is not yet implemented in the current release of PANIS. Once developed, a detailed description of the approach, along with its integration into the processing workflow, will be provided.

END OF DOCUMENT